The impact of soil land cover infiltration rates on flood modelling

A case study in Lomma Municipality (Sweden)

Joshua Friese

Swedish University of Agricultural Sciences, SLU
Faculty of Landscape Architecture, Horticulture and Crop Production Sciences
Department of Landscape Architecture, Planning and Management
Alnarp 2025

The impact of soil land cover infiltration rates on flood modelling: A case study in Lomma Municipality (Sweden)

Die Auswirkungen von Infiltrationsraten der Bodenbedeckung auf die Hochwassermodellierung

Joshua Friese

Supervisor:	**Abdulghani Hasan, Swedish University of Agricultural Sciences, Department of Landscape Architecture, Planning and Management**
Examiner:	Neil Sang, Swedish University of Agricultural Sciences, Department of Landscape Architecture, Planning and Management
Credits:	15
Level:	G2E
Course title:	Independent project in Landscape architecture
Course code:	EX1011
Programme/education:	Forest and Landscape
Course coordinating dept:	Department of Landscape Architecture, Planning and Management
Place of publication:	Alnarp
Year of publication:	2025
Copyright:	All featured images are used with permission from the copyright owner.
Keywords:	land use, land cover, soil infiltration rate, flooding

Swedish University of Agricultural Sciences
Faculty of Landscape Architecture, Horticulture and Crop
Production Sciences
Department of Landscape Architecture, Planning and Management

Publishing and archiving

Approved students' theses at SLU can be published online. As a student you own the copyright to your work and in such cases, you need to approve the publication. In connection with your approval of publication, SLU will process your personal data (name) to make the work searchable on the internet. You can revoke your consent at any time by contacting the library.

Even if you choose not to publish the work or if you revoke your approval, the thesis will be archived digitally according to archive legislation.

You will find links to SLU's publication agreement and SLU's processing of personal data and your rights on this page:

- https://libanswers.slu.se/en/faq/228318

☒ YES, I, Joshua Friese, have read and agree to the agreement for publication and the personal data processing that takes place in connection with this.

☐ NO, I/we do not give my/our permission to publish the full text of this work. However, the work will be uploaded for archiving and the metadata and summary will be visible and searchable.

Abstract

Flooding caused by extreme rainfall events has gained increased attention. To predict the potential extent and risks of such floods, dynamic flood model tools are crucial. However, flood simulation efforts lack standardized data on infiltration rates across different soil and land cover types. This study develops a standardized soil land cover (SLC) infiltration rate table, including both infiltration rate ranges and Manning coefficients. The table was constructed through a comprehensive literature review, analysis of the Soil Water Infiltration Global (SWIG) database, and logical estimations where data gaps existed. The aim of this table is to support urban planners, municipalities, and other hydrological modelers in more realistic flood simulations. The table was applied to a case study in Lomma Municipality (Sweden) using high-resolution GIS data and the dynamic flood model tool in ArcGIS Pro.

Flood simulations were conducted using minimum and maximum infiltration scenarios in a 10-year return rainfall event. Results show significant differences in flood extent depending on infiltration input, especially in flood depths greater than 30cm, where the area experiences ca. 33% less in the maximum infiltration scenario. Notably, SLCs on sandy soils with high infiltration showed substantial flood reduction potential, whereas clay-dominated areas remained flood-prone.

This study demonstrates the crucial role of accurate infiltration data in flood modelling and highlights the benefits of integrating soil and land cover characteristics. The developed SLC infiltration table offers a valuable planning tool for improving flood risk assessments and promoting climate-resilient urban design in Sweden and other regions with similar climate conditions.

Keywords: land use, land cover, soil infiltration rate, flooding

Table of contents

List of tables

List of figures

Abbreviations

DEM	Digital elevation model
Inf	Infiltration
Ksat	Saturated hydrated conductivity
LC	Land cover
LU	Land use
SLC	Soil land cover
SLU	Swedish University of Agricultural Sciences
SWIG	Soil Water Infiltration Global Database

1. Introduction

In recent years, global warming has led to more frequent heavy rainfall events and floods, with an upward trend for the future (Madsen et al. 2014). Sweden has been affected by several floods caused by heavy rainfall in recent years, for example, in Gävle in 2021 and Malmö, 2014 (Malmö stad 2024; S.V.T. Nyheter 2024). In the context of Sweden, the southwest coast is more frequently affected by the risk of flooding (Vieira Passos et al. 2024). Long-term water and flood management has gained importance and is demanded for sustainable landscape and urban planning. With the help of GIS tools, it is now possible to simulate extreme weather situations such as heavy rainfall in dynamic flood models to predict likely effects and minimize potential consequences. To make simulations as realistic as possible infiltration rate of soils and land cover is crucial.

Soil infiltration data is crucial for flood simulation and analysis. There are many sources about soil infiltration rates in that differ in big value ranges, which makes it hard for municipalities and other users to decide which one to use. This inconsistency complicates decision-making in flood risk assessment and sustainable land use planning.

To address these challenges, this study poses the following research question*: How do soil infiltration rates vary across different land use types, and how can a standardized infiltration rate table improve flood risk assessments?* By investigating this question, the study aims to close the gap between empirical infiltration data and its practical application in flood modelling.

Based on existing literature and observed variation in soil and land cover properties, this study hypothesizes that (1) *soil infiltration rates differ significantly between land use types*, and that (2) a *standardized infiltration rate table will improve the accuracy of flood simulations and facilitate better land use planning.*

This study is the first of its kind, creating a standardized soil land cover infiltration rate table, including Manning coefficients. Furthermore, this study demonstrates (1) how to use and prepare the soil land cover infiltration rate table for rainfall flood simulations and (2) the effect of these floods simulated with minimum and maximum infiltration. To achieve this aim, the study will:

1. Conduct a comprehensive literature review to compare and evaluate existing soil infiltration data, identifying variations and determine their sources.

2. Classify infiltration rates based on soil type and land cover in a combined soil land cover infiltration rate table to establish clear guidelines for their application in flood simulations.
3. Apply the table in a case study of Lomma Municipality to analyze flood outcomes under different infiltration scenarios.

This research will provide municipalities, urban planners, and hydrological modelers with a scientifically grounded reference table of soil infiltration rates and Manning coefficients, facilitating more accurate flood simulations and land use planning.

In this study, the Manning coefficient is not applied to the flood modelling, as ArcGIS Pro (flood modelling software) does not need Manning coefficients due to its algorithm. However, the Manning coefficients can be used for future reference in flood modelling for programs requiring the coefficients.

2. Background

2.1 Flood risk management in Sweden and Lomma municipality

Flood risk management in Sweden is led by a decentralized governance structure. The Swedish legal framework places the main responsibility for flood risk mitigation on municipalities (Becker 2021). This means that local governments are expected to take care of risk assessments, implement preventative strategies, as well as coordinate emergency responses on their own.

Lomma Municipality is vulnerable to coastal flooding. As part of its flood preparedness efforts, the municipality commissioned a detailed flood risk mapping study of the Höje å river and Önnerupsbäcken watercourse (SWECO 2009). The study looked at flooding under both current conditions and future sea level rise, simulating 100-year flood events with sea levels rising by +1.25 m and +1.89 m—the second value matching projections for the year 2100. Results show that natural land cover and the Örestad golf course in the upstream area of Höje Å are affected (SWECO 2009). Importantly, the report recommended further investigation of flood risks caused by extreme rainfall events—something that was not the primary focus of their modelling. This gap is directly addressed in this paper, which applies high-resolution infiltration data to simulate flooding in the same watershed under intense rainfall conditions. By integrating soil and land cover-based infiltration rates into flood modelling, this thesis builds on and complements the SWECO study, offering new insights for municipal planning and stormwater management in Lomma.

2.2 Factors influencing infiltration rates

The extent of flooding is essentially determined by soils physical properties. Soil structure, depth, permeability and organic matter directly influence the infiltration rates of the soil (Saco et al. 2021). The pore size of soils is the most important soil property regarding infiltration rate. Soils with large pores like sandy soils have higher infiltration and therefore produce lower runoff, whereas clay soils who have small pores produce higher runoff (Saco et al. 2021).

Secondly, land use is an important factor regarding soil infiltration rates. Research has shown that changes in land use can significantly affect soil physical properties, such as compaction, porosity, and organic matter content, which in turn influence infiltration capacity (Fu et al. 2000; Shukla et al. 2003; Yimer et al. 2008; Sun et al. 2018). These changes can either enhance or reduce the ability of

soil to absorb water, depending on whether the new land use increases sealing like artificial surfaces, or promotes infiltration, such as through natural land cover types. In the context of this thesis, understanding how different land use types affect infiltration supports the development of a standardized infiltration rate table that accounts for both soil type and land cover.

Another factor influencing the infiltration process is the topography. A study by Fox et al. (1997) demonstrated that the infiltration rate decreases as the slope angle increases. This finding highlights the role of elevation in areas where water infiltrates, with steeper slopes potentially leading to less water infiltrating the soil. Regarding the flat topography in the study area, it will be interesting to see if small changes in slope still have some effect on infiltration.

2.3 Manning's coefficient

The Manning coefficient (n) describes the roughness or smoothness of various land cover types (also known as *Manning roughness coefficient*). From this, the runoff speed of water on the surface can be calculated and therefore is an important factor in hydrological calculations (Ye et al. 2018). Some dynamic flood modelling tools, such as PluvioFlow, require Manning coefficients in order to perform the simulation. In this study, the ArcGIS Pro dynamic flood modelling tool is used, which does not require Manning coefficients as input, as the program calculates runoff with a different algorithm.

3. Methods

3.1 Literature review

Literature review has been performed in order to find suitable values for infiltration rates and manning coefficients across different land cover and soil types and their manning coefficient. Scientific databases such as “Scopus”, “Google Scholar” and “jstor” has been searched by keyword searches such as: (“stormwater” AND “infiltration” AND “land use” OR “land cover”), (“rainfall” AND “infiltration” AND land use” OR “land cover”), (“infiltration” AND “land use” or “land cover”) and (“manning coefficient” AND “land cover” OR “land use”).

3.2 SWIG database

The Soil Water Infiltration Global database (SWIG) has been used to find infiltration rates. The database contains infiltration rate measurements from 1976-2017 from all over the world including information about the land use and soil type (Rahmati et al. 2018). SWIG database was processed and filtered with R-Studio: the database was grouped by “Texture Class” and “Landuse (classified)” and the saturated hydrated conductivity (Ksat in cm/hr) was summarised by number of counts (n), mean Ksat and median Ksat value. In addition, data that doesn’t contain Ksat values and/or “Landuse (classified)” values were erased. The Ksat value was transformed from cm/hr to mm/hr. The code applied in R-Studio can be seen in Appendix 1, Figure 1.

3.3 Study area

The study area is located within Lomma municipality in Skåne County, Sweden. Lomma municipality is within the temperate oceanic climate zone. Lomma receives rainfall year-round, with an average monthly precipitation of 43 mm. In Augst most precipitation occurs with 54 mm, whereas March is the most with lowest precipitation 29 mm. The average temperature in Lomma is 8.5 °C, with January and February as the coldest months with 1°C on average and July and August as the warmest month with 17°C. The topography of Lomma is predominantly flat, with minimal elevation variation across the study area (Figure 3).

The area is 448ha and part of the Höje Å watershed. The Höje Å river flows through Lomma and into the Baltic Sea. Main soil type within are clay soils (56%) and sandy soils (37%). Silty soils cover less than 1% and 6% are water

bodies (Figure 1). From the centre to the south, as well as in the west where the Höje Å munches into the ocean, the watershed is characterised by urban land cover, consisting mainly of buildings and paved roads (Figure 2). However, plenty of small green spaces can be found within the urbanised areas. In the north of the watershed is much land covered by natural surfaces, such as shallow and dense vegetation, water and fields (Figure 2).

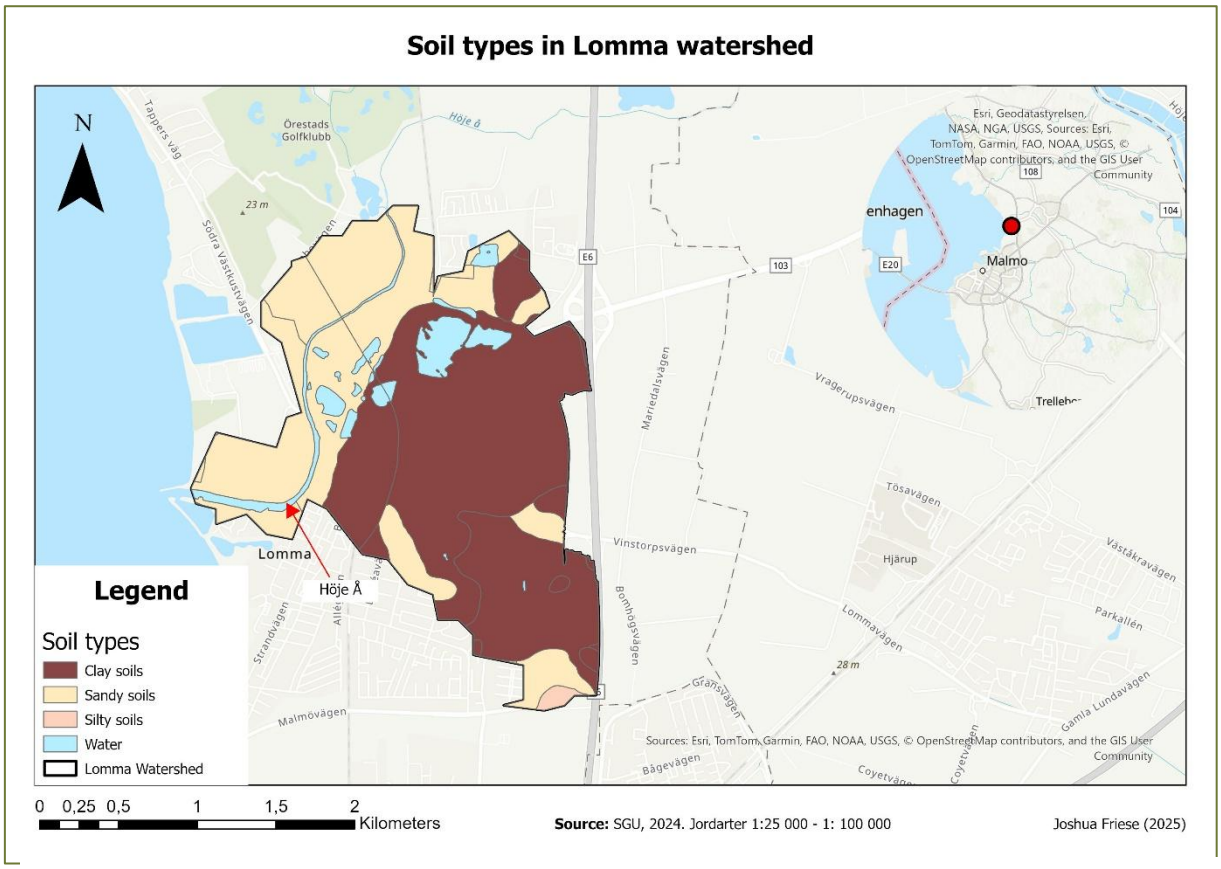

Figure 1. Map of soil types within Lomma watershed.

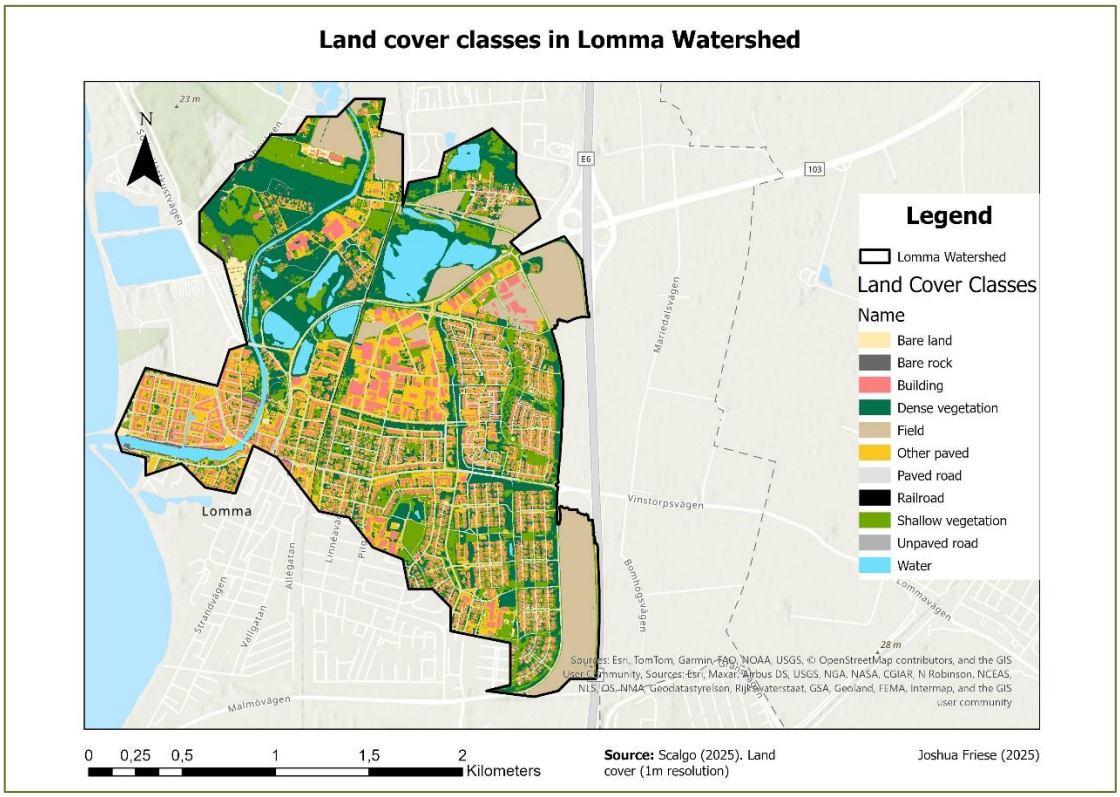

Figure 2. Map of land cover classes within Lomma watershed. Downloaded from Scalgo (2025).

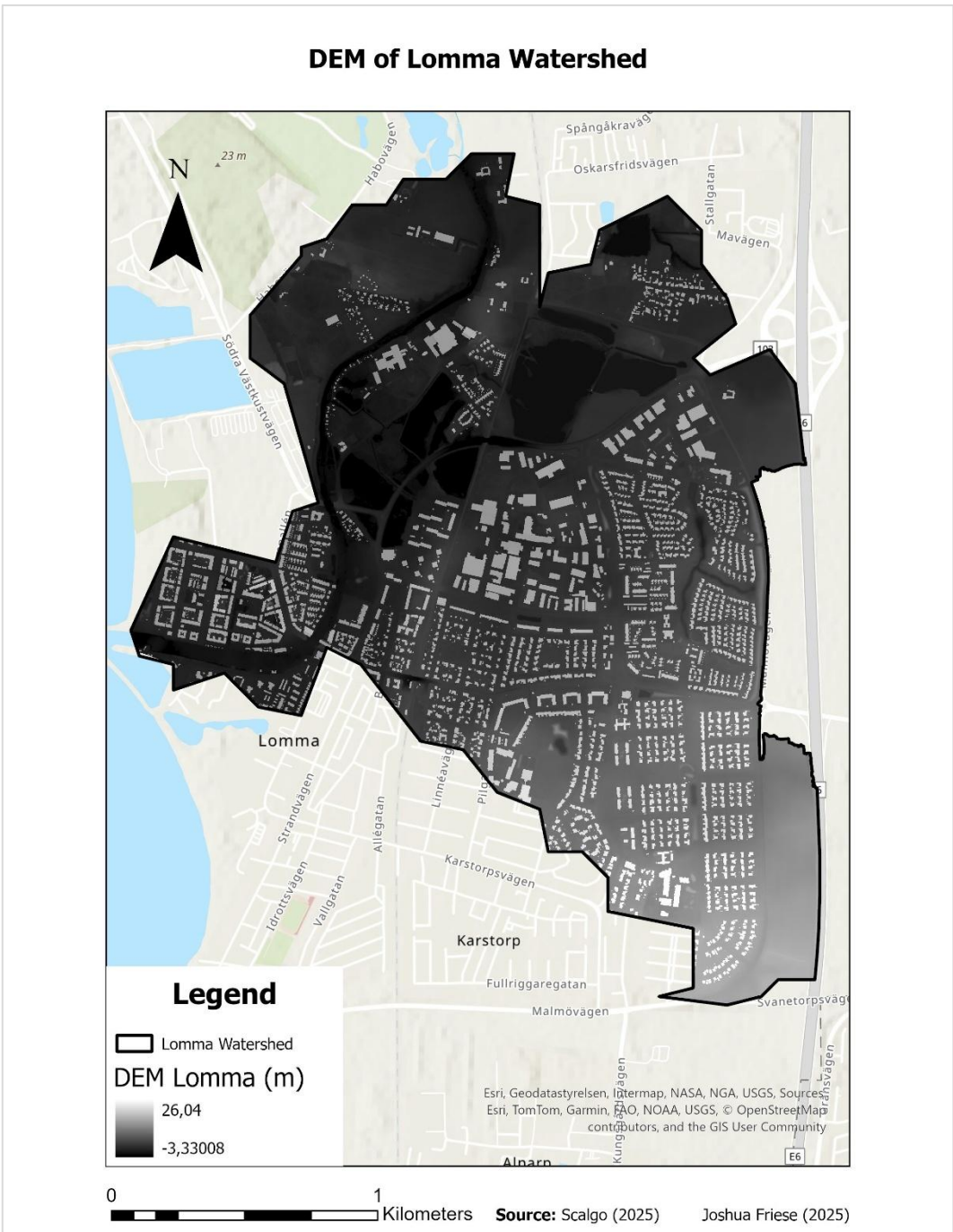

Figure 3. Digital elevation model (DEM) of Lomma watershed. Downloaded from Scalgo (2025)

3.4 Guidelines for infiltration rates and soil groups

Soil types were divided into three groups sandy soils, silty soils and clay soils based on their hydrological soil group, as it can be seen in Figure 4 (Sayl et al. 2017). Sandy clay loam was grouped into clay soils. Combined with the Green-Ampt parameter table (Table 1) by Rawls & Brakensiek (1982), Rawls et al. (1982), Gowdish & Muñoz-Carpena (2009) estimates for maximum infiltration rates have been defined. Maximum infiltration for sandy soils is 236 mm/hr, 23 mm/hr for silty soils, and 4 mm/hr for clay soils.

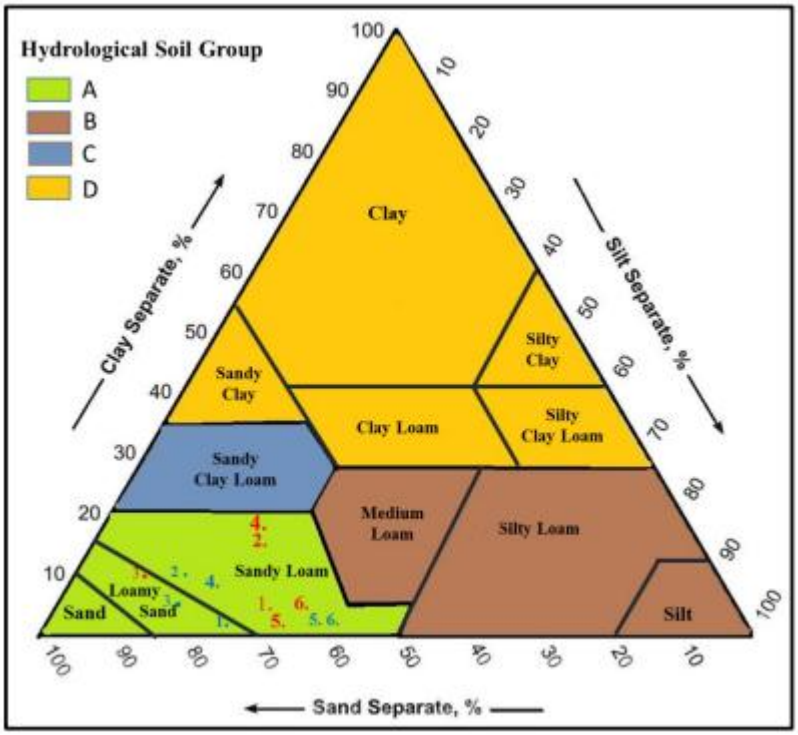

Figure 4. Soil type triangle and their hydrological soil group (Sayl et al. 2017)

Table 1. Green-Ampt parameter table by Rawls & Brakensiek (1982), Rawls et al. (1982), Gowdish & Muñoz-Carpena (2009).

Soil Texture	Residual Water Content (-)	Wilting Point (-)	Field Capacity (-)	Total Porosity (-)	Pore-size Distribution Index (-)	Saturated Hydraulic Conductivity (cm/hr)	Wetting Front Suction(cm)
Silt loam	0.015	0.133	0.261	0.501	0.234	0.68	32.96 – 40.4
Sand	0.02	0.033	0.048	0.437	0.694	21.0 – 23.56	9.62 – 10.6
Loam	0.027	0.117	0.20	0.463	0.252	1.32	17.50 – 31.5
Loamy sand	0.035	0.055	0.084	0.437	0.553	5.98 – 6.11	11.96 – 14.2
Silty clay loam	0.040	0.208	0.30	0.471	0.177	0.15 – 0.20	53.83 – 58.1
Sandy loam	0.041	0.095	0.155	0.453	0.378	2.18 – 2.59	21.53 – 22.2
Silty clay	0.056	0.250	0.317	0.479	0.150	0.09 – 0.10	57.77 – 64.7
Sandy clay loam	0.068	0.148	0.187	0.398	0.319	0.30 – 0.43	44.9 – 53.83
Clay loam	0.075	0.197	0.245	0.464	0.242	0.20 – 0.23	40.89 – 44.6
Clay	0.09.	0.272	0.296	0.475	0.165	0.06	62.25 – 71.4
Sandy clay	0.109	0.239	0.232	0.430	0.223	0.12	46.65 – 63.6

3.5 Data processing and flood modelling

Land cover data and digital elevation model including buildings (DEM) have been accessed and downloaded from Scalgo as raster datasets in 1-meter resolution (Scalgo 2025). The land cover raster from Scalgo contains 15 land cover classes (see Figure 2). Soil type vector data (Jordarter 1:25 000-1:100 000) has been accessed and downloaded from Sveriges geologiska undersökning (SGU 2024). In the next step, soil types of this vector data have been categorized into clay soils, silty soils, sandy soils, and water with the field calculator in ArcGIS Pro (Code in Appendix 2). Subsequently, the soil type vector has been rasterized and combined with the land cover raster from Scalgo to form the *SLC I*. The *SLC I* contains 39 soil type-land use combinations, which have been matched with the *soil land cover infiltration table* (Table 2), resulting in *SLC II* (see Table 6). Additionally, minimum and maximum infiltration rates have been added to *SLC II*.

The DEM including buildings has been set to ground layer, minimum and maximum infiltration rasters have been input for the infiltration raster in the flood simulation tool of ArcGIS Pro. A rainfall event with 90 mm/hr precipitation for 15 minutes and 15 minutes “cool-down” with no precipitation (in total 22,5 mm) has been performed once for minimum and once for maximum infiltration. This precipitation is in the range of a 10-year return event according to the study of

Poschlod et al. (2021). The full workflow of data handling can be seen in Figure 5.

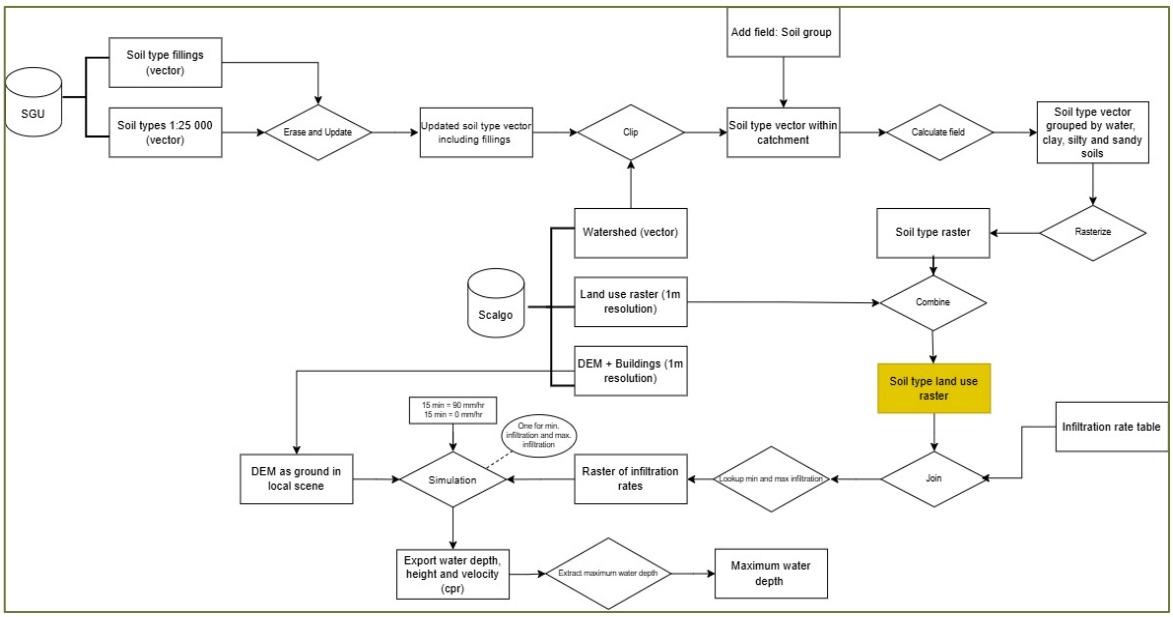

Figure 5. Flowchart of dataset processing and flood modelling

4. Results

4.1 Soil land cover infiltration table and Manning coefficient

The soil land cover infiltration table (Table 2) covers 24 soil land cover classes. The infiltration rates are presented in mm/hr. Infiltration for different land use classes on sandy soils was the highest, followed by silty soils, and clay soils with the lowest infiltration (Table 2). Infiltrations of artificial land uses such as *buildings*, *roads*, and *railroads* seal the surface layer and therefore have low infiltration and are not dependent on underlying soil types (Table 2).

For natural SLCs, *rain garden* has the highest infiltration, followed by *forest-high vegetation*, *field-agricultural land*, and *bare land-peat* (Table 2). *Water* has the lowest infiltration, followed by *Bedrock (exposed)* and *wetlands/marsh*. *Bare land-compacted* has a big range of infiltration, as this SLC includes all three soil groups (Table 2). The biggest infiltration range of all SLCs has *bare land-peat*.

In general, infiltration rates among natural land use classes differ a lot, even in the same soil group. The same applies to same SLCs on different soil groups (Table 2).

The Manning coefficients are lowest amongst the artificial surfaces as their surfaces are smoother compared to natural surfaces (Table 2). The lowest n value and range has the SLC *building-roof*, whereas *wetlands/marsh* has the highest n value (Table 2). The Manning coefficients are dependent on the land cover type and do not differ within the same land cover class on the soil type.

Table 2. Range of infiltration rates (mm/hr) and Manning coefficients for soil land cover classes

LU-LC	Soil	SLC	min inf	max inf	min n	max n
Building - roof	///	Building - roof	1	1	0.01	0.01
Building - Green roof	///	Building - Green roof	33.75	41.25	0.1	0.1
Roads - Pavement – Asphalt	///	Roads - Pavement - Asphalt	0	1	0.01	0.013
Roads - Pavement – Bricks	///	Roads - Pavement - Bricks	0.5	5	0.01	0.013
Roads - Pavement – permeable	///	Roads - Pavement - permeable Asphalt	15	30	0.01	0.013
Roads - Unpaved	///	Roads - Unpaved	1.5	20	0.03	0.035
Roads - Gravel	Gravel	Roads - Gravel	5	25	0.025	0.035
Railroads	///	Railroads	0	1	0.02	0.035

Forest - high vegetation	Clay	Forest or high vegetation on clay soil	2.25	2.7	0.08	0.2
Forest - high vegetation	Silt	Forest or high vegetation on silty soil	16.5	20	0.08	0.2
Forest - high vegetation	Sand	Forest or high vegetation on sandy soil	176.3	211.5	0.08	0.2
Grass - lawn - low vegetation	Clay	Grass or lawn - low vegetation on clay soil	0.3	1.8	0.025	0.05
Grass - lawn - low vegetation	Silt	Grass or lawn - low vegetation on silty soil	2.2	13.2	0.025	0.05
Grass - lawn - low vegetation	Sand	Grass or lawn - low vegetation on sandy soil	23.5	136	0.025	0.05
Field - agricultural land	Clay	Field - agricultural land on clay soil	1.5	2.1	0.02	0.05
Field - agricultural land	Silt	Field - agricultural land on silty soil	11	15.4	0.02	0.05
Field - agricultural land	Sand	Field - agricultural land on sandy soil	117.5	164.5	0.02	0.05
Bare land	Bedrock	Bedrock (Exposed)	0	1	0.03	0.05

Bare land	Any compacted	Bare land-compacted	1.2	50	0.04	0.05
Bare land	Peat	Bare land-peat	100	150	0.04	0.05
Bare land	Rocks and gravel	Bare land rocks and gravel	30	50	0.03	0.05
Water	///	Water	0	0	0.025	0.05
Wetlands / Marsh (With Vegetation)	///	Wetlands / Marsh (With Vegetation)	0.3	3	0.2	0.3
Rain garden	Sand	Raingarden	188	211.5	0.15	0.2

4.2 Results from SWIG database and sources of soil land cover infiltration table

The SWIG database contains soil infiltration rates for 6 in this paper relevant natural land cover classes (Table 3). In total, 1334 infiltration rates have been found in the SWIG database, 48% of land cover classes on sandy soils, 29% on silty soils, and 22% on clay soils (Table 3). Most infiltration rates have been found for agricultural land cover across all soil types (65%) (Table 3). These infiltration rate ranges (Table 4) have influenced the final infiltration ranges for SLC *Fields- agricultural land* (Table 5). In addition, SWIG infiltration rates for *grass - lawn - low vegetation* on sandy and silty soils have been considered in the soil land cover infiltration table (Table 5). Land cover classes with few counts of infiltration rates, such as urban soils and shrubs, have not been considered later. Same for land cover classes with big ranges, such as forests on sandy and clay soils, urban soils, and shrubs (Table 4).

Table 3. Counts of SWIG infiltration rates on natural land cover classes

Land cover	Sandy soils	Silty soils	Clay soils
Agriculture	392	281	197
Forest	49	23	21
Pasture	108	36	23
Grass	23	45	46
Urban soil	69	4	3
Shrub	10	3	1
Total	**651**	**392**	**291**

Table 4. Infiltration rate ranges (in mm/hr) per land cover and soil type from SWIG database

Land cover	Sandy soils	Silty soils	Clay soils
Agriculture	56-150	32-43	28-150
Forest	5.5-9000	0-0.7	910-5250
Pasture	21.9-552.6	43-51.1	0-61
Grass	18.6-136.1	10-21.7	286-1776
Urban soil	110-2240	101-339	154
Shrub	0-4010	0	0

Sources for infiltration rates vary between single sources, SWIG database and estimations (Table 5). The majority of artificial land cover classes, such as buildings and roads, have been determined by estimates (Table 5). In total, 48% of all infiltration rates are estimates (Table 5). For Manning coefficient, 40 % derive from the “HEC-RAS River Analysis System: 2D Modeling User’s Manual. Version 5.0” by (U.S. Army Corps of Engineers 2021), another 40% from estimates, and 20% from Ni et al. (2021) (Table 5).

Table 5. Sources for infiltration rates and manning coefficients for soil land cover table

LU-LC	Soil	SLC	Infiltration-Source	Manning-Source
Building - roof	///	Building - roof	Estimate	Estimate
Building - Green roof	///	Building - Green roof	Bondì et al. (2023)	Estimate
Roads - Pavement - Asphalt	///	Roads - Pavement - Asphalt	Estimate	Ni et al. (2021)
Roads - Pavement - Bricks	///	Roads - Pavement - Bricks	Estimate	Ni et al. (2021)
Roads - Pavement - permeable	///	Roads - Pavement - permeable Asphalt	Roseen et al. (2012)	Ni et al. (2021)
Roads - Unpaved	///	Roads - Unpaved	Estimate	Estimate
Roads - Gravel	Gravel	Roads - Gravel	Estimate	Estimate
Railroads	///	Railroads	Estimate	Estimate

Forest - high vegetation	Clay	Forest or high vegetation on clay soil	Estimate	U.S. Army Corps of Engineers (2021)
Forest - high vegetation	Silt	Forest or high vegetation on silty soil	Sauer et al. (2005)	U.S. Army Corps of Engineers (2021)
Forest - high vegetation	Sand	Forest or high vegetation on sandy soil	Estimate	U.S. Army Corps of Engineers (2021)
Grass - lawn - low vegetation	Clay	Grass or lawn - low vegetation on clay soil	Estimate	U.S. Army Corps of Engineers (2021)
Grass - lawn - low vegetation	Silt	Grass or lawn - low vegetation on silty soil	SWIG; Mueller & Thompson (2009); Wikantyasa & Kusumandari (2022)	U.S. Army Corps of Engineers (2021)
Grass - lawn - low vegetation	Sand	Grass or lawn - low vegetation on sandy soil	SWIG	U.S. Army Corps of Engineers (2021)
Field - agricultural land	Clay	Field - agricultural land on clay soil	SWIG	U.S. Army Corps of Engineers (2021)
Field - agricultural land	Silt	Field - agricultural land on silty soil	SWIG	U.S. Army Corps of Engineers (2021)

Field - agricultural land	Sand	Field - agricultural land on sandy soil	SWIG, Amami et al. (2021)	U.S. Army Corps of Engineers (2021)
Bare land	Bedrock	Bedrock (Exposed)	Estimate	Estimate
Bare land	Any compacted	Bare land-compacted	Estimate	Estimate
Bare land	Peat	Bare land-peat	Estimate	Estimate
Bare land	Rocks and gravel	Bare land-rocks and gravel	Estimate	Estimate
Water	///	Water	(Scalgo 2025)	U.S. Army Corps of Engineers (2021)
Wetlands / Marsh (With Vegetation)	///	Wetlands / Marsh (With Vegetation)	Estimate	Estimate
Rain garden	Sand	Raingarden	Venvik & Boogaard (2020)	Estimate

4.3 Reclassification of previous SLCs to thesis SLC scheme

The *SLC I* has been classified with the SLC table from this paper, including infiltration rates and Manning coefficient, which can be seen in Figure 6. The *SLC II* has been decided on *SLC I* combinations and reviewing satellite imagery. In total, the 39 previous SLC combinations were assigned to 16 of a possible 24 SLCs available in this thesis (Table 6).

Many of the SLCs from *SLC I* could easily be classified with the SLCs from this paper, such as when *SLC I* included “Field”, “Shallow vegetation”, or “Dense vegetation” (Table 6). When *SLC I* included “Water” or “other paved” reviewing with satellite imagery was necessary to assign to *SLC II*. In Table 6, *OBJECTID 4* did not get the full range of infiltration from Table 2 because the infiltration rate range of SLC “Bare land compacted” (Table 2) considers all kinds of soil groups. A relatively high infiltration rate has been assigned to *OBJECTID 4*, as the underlying soil type is a sandy soil (Table 6). No value was assigned to *OBJECTID 25* and *32*, as no clear land cover could be determined after examining the satellite images, even taking into account neighboring cells, due to their size corresponding to a single pixel (1m x 1m) (Table 6). The resulting SLC raster can be seen in Figure 6, which is more detailed than the land cover raster from Scalgo (Figure 2).

In Figure 6, we can see that the urbanized area in the center of the watershed contains a lot of natural land cover types surrounded by buildings and road constructions. Furthermore, we see that most of the water bodies in the study area are surrounded by forests (Figure 6). Bare land and field cover can be found along the borders of the study area in the north, as well as in the south-east (Figure 6). Notable as well is that in most cases, bigger buildings are surrounded by roads.

Table 6. SLC I matched with *SLC II* and the corresponding Infiltration rates and Manning coefficients

OBJECTID	*SLC I* (Soil type, Scalgo landcover)	*SLC II* (SLC classes from my table)	Min Inf	Max inf	min n	max n
1	Sandy, Field	**Field - agricultural land on sandy soil**	117.5	164.5	0.02	0.05
2	Sandy, Shallow vegetation	**Grass or lawn - low vegetation on sandy soil**	23.5	136	0.025	0.05
3	Sandy, Dense vegetation	**Forest or high vegetation on sandy soil**	176.3	221.5	0.08	0.2
4	Sandy, bare land (compacted)	**Bare land compacted**	20	50	0.04	0.05
5	Sandy other paved	**Roads - Pavement - Asphalt**	0	1	0.01	0.013
6	Sandy, Building	**Building - roof**	0.5	1	0.01	0.01
7	Water, Water	**Water**	0	0	0.2	0.3
8	Water, Shallow vegetation	**Water**	0	0	0.2	0.3
9	Sandy, Water	**Water**	0	0	0.2	0.3
10	Sandy, Rare rock	**Bare land rocks and gravel**	30	50	0.03	0.05
11	Sandy, Paved road (Asphalt)	**Roads - Pavement - Asphalt**	0	1	0.01	0.013
12	Water, Dense vegetation	**Water**	0	0	0.2	0.3
13	Water, Bare land	**Water**	0	0	0.2	0.3
14	Sandy, Unpaved road	**Roads - Unpaved**	1.5	20	0.03	0.035
15	Clay, Dense Vegetation	**Forest or high vegetation on clay soil**	2.25	2.7	0.08	0.2
16	Clay, Shallow Vegetation	**Grass or lawn - low vegetation on clay soil**	0.3	1.8	0.025	0.05
17	Clay, Other paved (asphalt)	**Roads - Pavement - Asphalt**	0	1	0.01	0.013

18	Clay, Bare rock (compacted maybe)	**Bare land compacted**	1.2	3	0.04	0.05
19	Clay bare land	**Grass or lawn - low vegetation on clay soil**	0.3	1.8	0.04	0.05
20	Clay building	**Building - roof**	0.5	1	0.01	0.01
21	Sandy railroad	**Railroads**	0	1	0.02	0.035
22	Clay paved road	**Roads - Pavement - Asphalt**	0	1	0.01	0.013
23	Clay, Field	**Field - agricultural land on clay soil**	1.5	2.1	0.02	0.05
24	Clay, Railroad	**Railroads**	0	1	0.02	0.035
25	Sandy, Snow-Ice	**No value**	0	0	0	0
26	Clay, Water	**Water**	0	0	0.2	0.3
27	Water, Other paved	**Roads - Pavement - Asphalt**	0	1	0.01	0.013
28	Water, Bare rock	**Water**	0	0	0.2	0.3
29	Water, Building	**Building - roof**	0.5	1	0.01	0.01
30	Clay, Unpaved road	**Roads - Pavement - Asphalt**	0	1	0.01	0.013
31	Water, Paved road (Bridges)	**Roads - Pavement - Asphalt**	0	1	0.01	0.013
32	Clay, Snow-Ice	**No value**	0	0	0	0
33	Silty other paved	**Roads - Pavement - Asphalt**	0	1	0.01	0.013
34	Silty shallow	**Grass or lawn - low vegetation on silty soil**	2.2	13.2	0.025	0.05
35	Silty paved road	**Roads - Pavement - Asphalt**	0	1	0.01	0.013
36	Silty dense	**Forest or high vegetation on silty soil**	16.5	20	0.08	0.2

37	Silty Field	**Field - agricultural land on silty soil**	11	15.4	0.02	0.05
38	Silty bare land	**Forest or high vegetation on silty soil**	16.5	20	0.04	0.05
39	Silty building	**Building - roof**	0.5	1	0.01	0.01

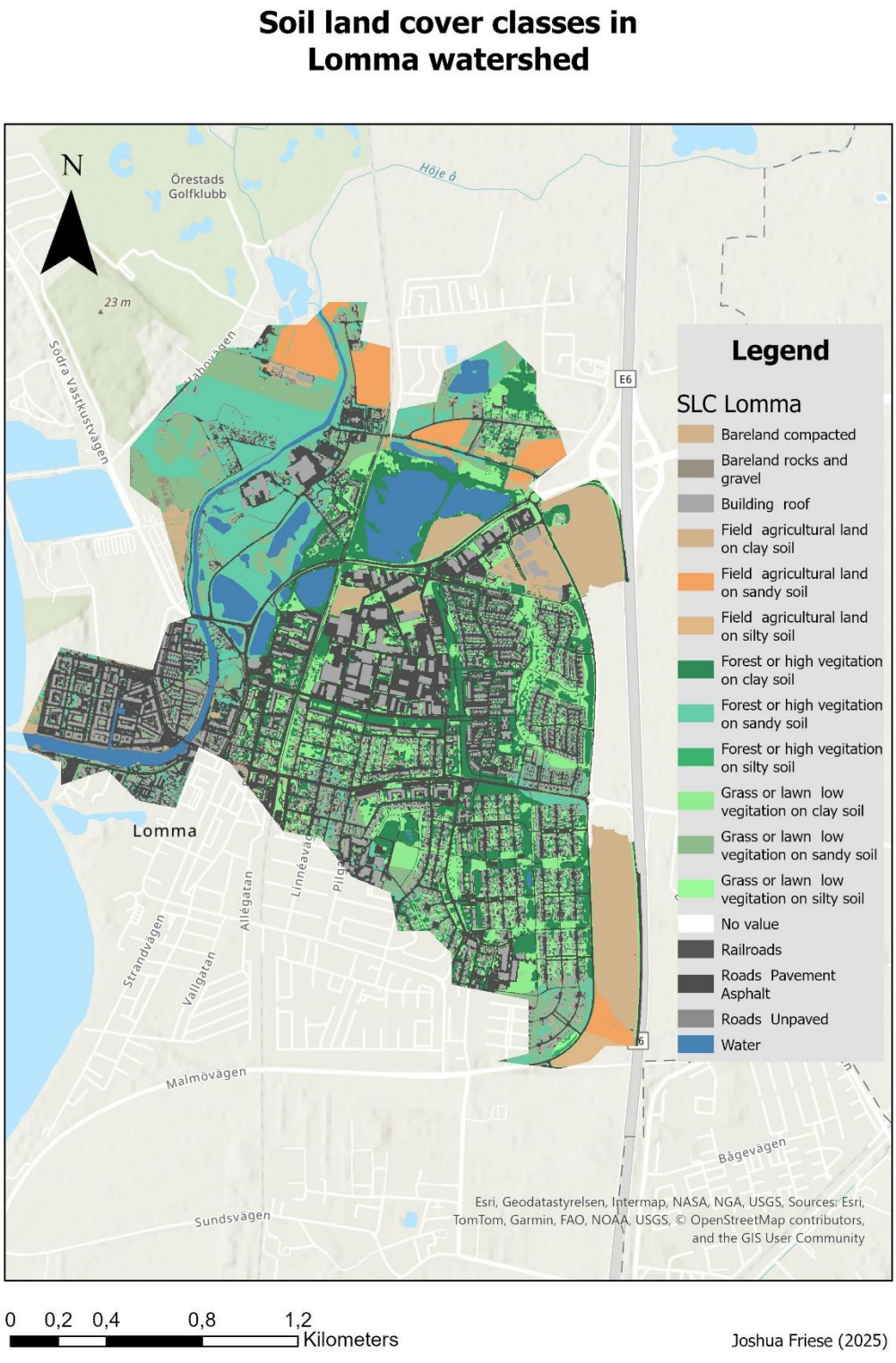

Figure 6. SLC II map of Lomma according to SLC Thesis scheme

4.4 Flooding simulation with minimum and maximum infiltration

After performing the flood simulations with minimum and maximum infiltration scenarios for the Lomma watershed, the maximum water depth of the rainfall event was extracted for each case (Figure 7). Both simulations affected similar areas, with most flooded zones exhibiting water depths below 10 cm. The urbanized areas within the watershed show nearly identical flood extents in both scenarios, with several patches where the maximum water depth reaches up to 30cm (Figure 7). In the southern part of the watershed, there is also an urbanized area where the maximum water depth exceeds the threshold of 30cm (Figure 6), although this area is slightly elevated compared to the rest of the study area and contains natural land cover. Furthermore, many of the water bodies in the study area appear to be minimally flooded (Figure 7). For rural areas, which can be found in the north of the watershed, we see more areas with higher water depth by minimum infiltration compared to maximum infiltration (Figures 7,8, and 9).

This also aligns with the results from Table 7. In the minimum infiltration scenario, 2.6ha of *Forest or high vegetation on sandy soil* experiences maximum water depth higher than 30cm, followed by *Roads Pavement Asphalt* with 2.27ha. For maximum infiltration*, Roads Pavement Asphalt* experience the most water depth >30cm with 2.3ha followed by *Forest or high vegetation on clay soil* 1.32ha, and 1.18ha on *grass or lawn low vegetation on clay soil*. In general, we see that 9ha by minimum infiltration of the whole watershed experience higher water depth >30cm, compared to 6ha by maximum infiltration (Table 7). *Forest or high vegetation on sandy soil* are main contributors to this difference.

In general, the average change in difference of affected area from minimum infiltration to maximum infiltration across all affected SLCs is ca. -21%. The biggest difference is between *Forest or high vegetation on sandy soil* (-93%) and *Grass or lawn low vegetation on sandy soil* (-63%) (Table 7). SLCs on clay soils experience minor changes from minimum to maximum infiltration scenario but remain flood-prone (Table 7).

The difference in maximum water depth between the two infiltration scenarios predominantly ranged from 1 to 10 cm (Figures 8 and 9). These differences were observed primarily in water bodies, as well as in *grass, lawn–low vegetation*, and *agricultural fields on sandy soils* situated in the northern part of the watershed (Figure 8). These areas coincide with topographic depressions visible in the DEM (Figure 9), where surface water tends to accumulate. In contrast, slightly elevated

areas within the watershed (in the south of the watershed) exhibited minimal differences in maximum water depth between the two simulations, except small depressions in the area (Figure 9).

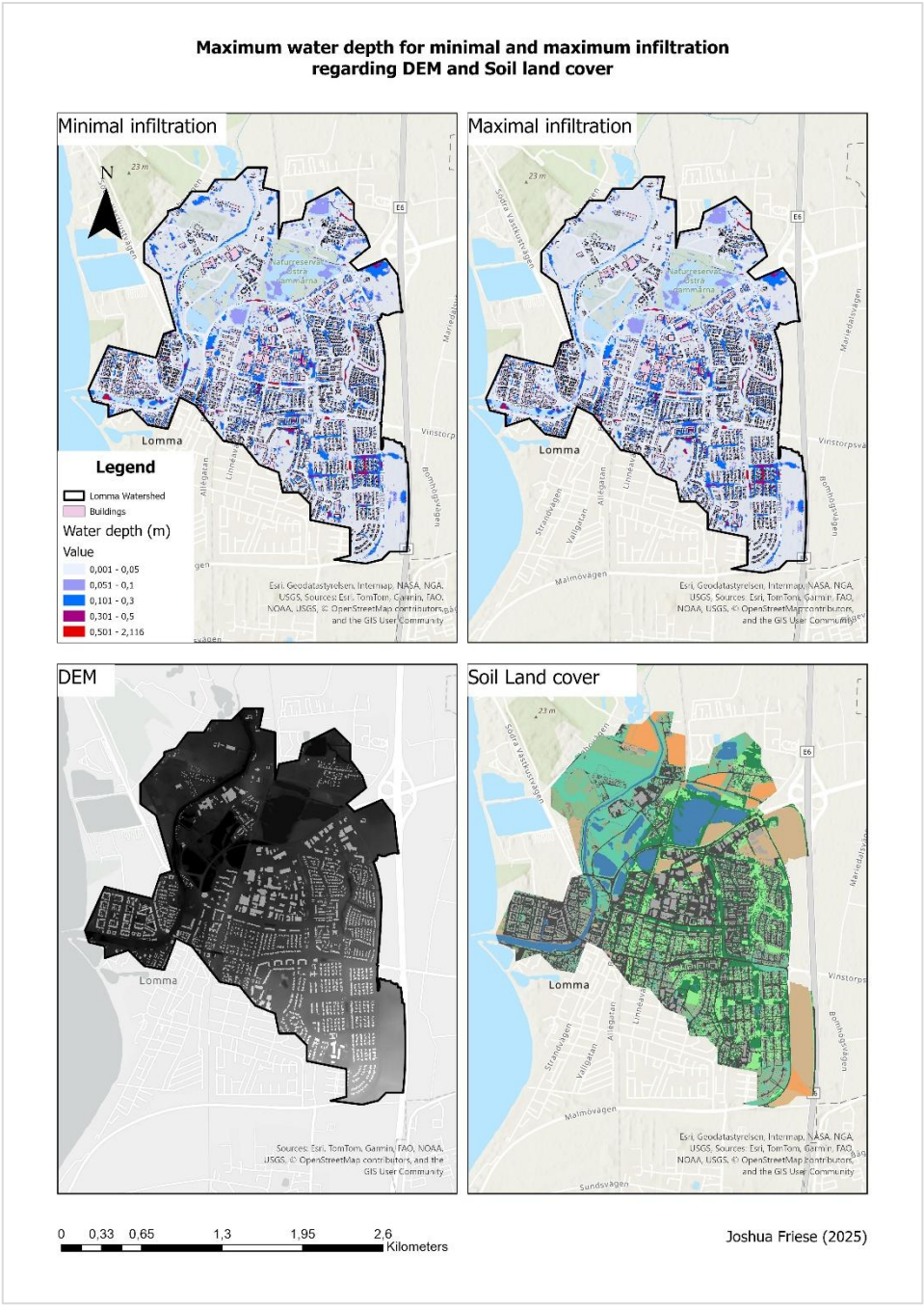

Figure 7. Maximum water depth for minimum and maximum infiltration rates after performing rainfall simulation with 90 mm/hr precipitation for 15 minutes and 15 minutes cool down (in total 22.5 mm)

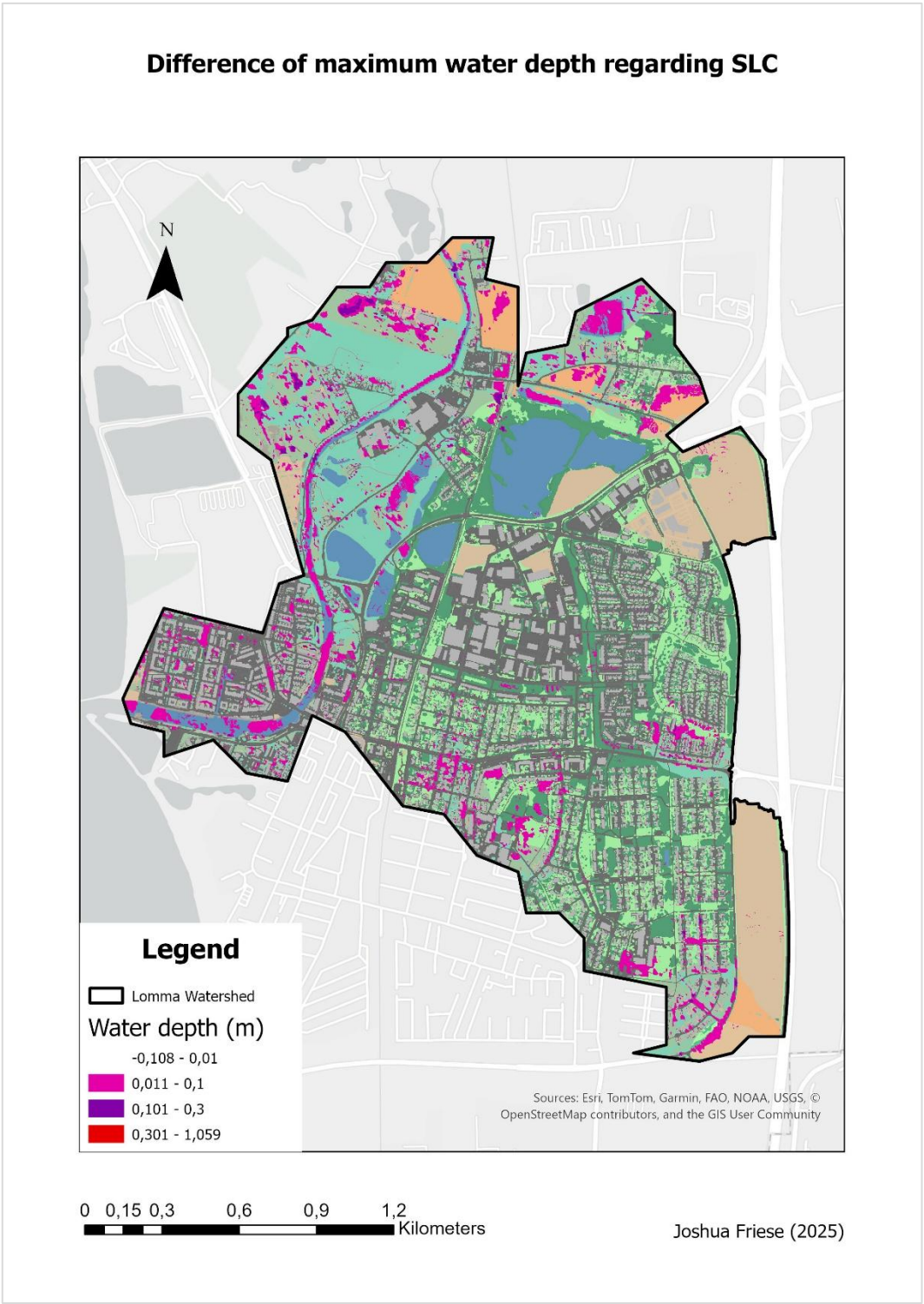

Figure 8. Difference of maximum water depth between minimum and maximum infiltration simulation regarding SLC (Minimum infiltration - Maximum infiltration).

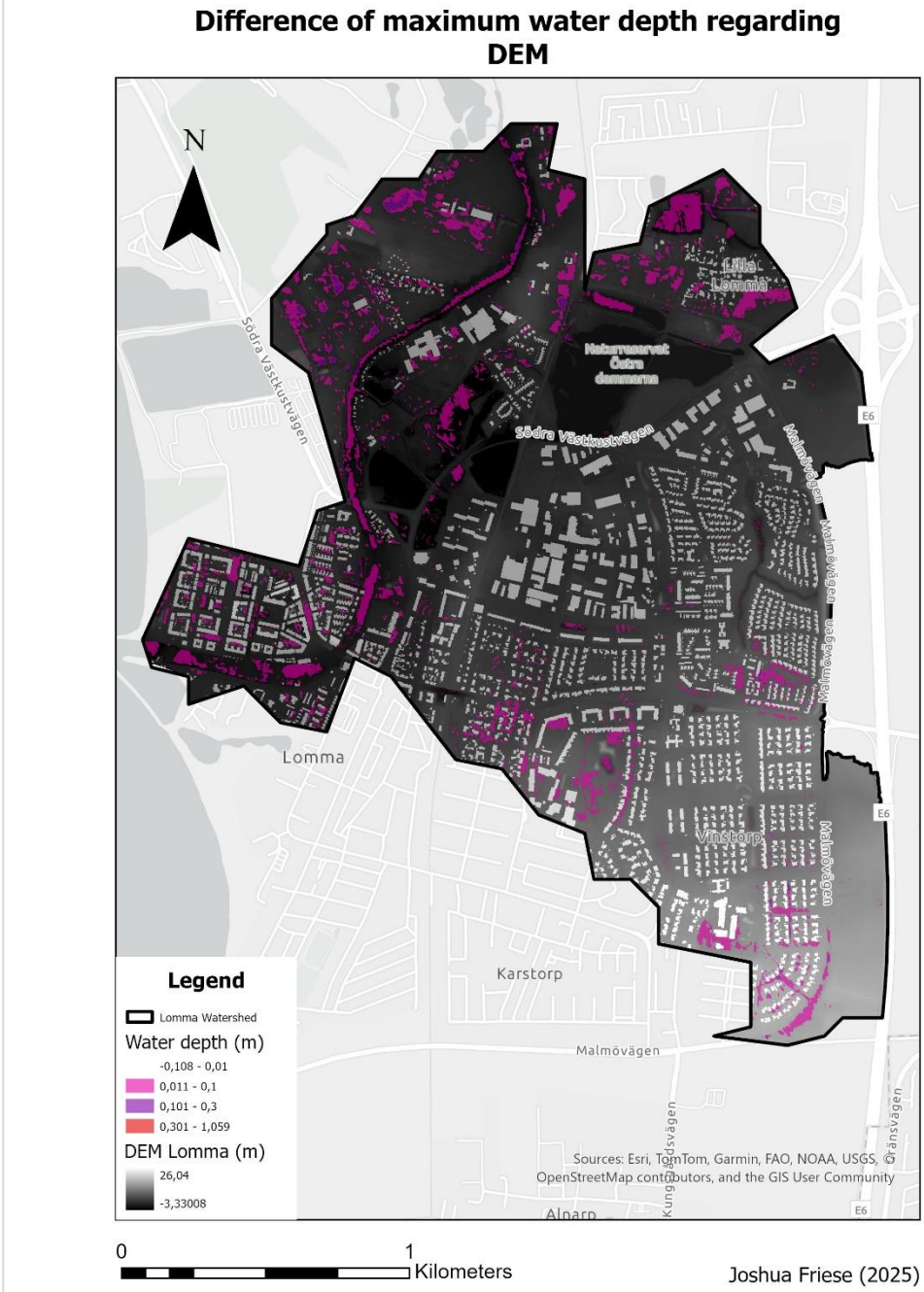

Figure 9. Difference of maximum water depth between minimum and maximum infiltration simulation regarding DEM (Minimum infiltration - Maximum infiltration). Where in the topography do we see a difference of water depth between the scenarios.

Table 7. Area (ha) experiencing maximum water depth >30cm per SLC, for minimum and maximum infiltration scenarios

SLC	Minimum Infiltration (ha)	Maximum Infiltration (ha)	% change (Min to Max infiltration)
Forest or high vegetation on sandy soil	2,6423	0,16	-93,94466942
Roads Pavement asphalt	2,2753	2,13	-6,385971081
Forest or high vegetation on clay soil	1,3754	1,32	-4,027919151
Grass or lawn low vegetation on clay soil	1,2412	1,18	-4,930712214
Water	0,8564	0,63	-26,43624475
Field agricultural land on clay soil	0,2901	0,28	-3,481558083
Grass or lawn low vegetation on sandy soil	0,1398	0,05	-64,23462089
Building roof	0,1377	0,21	52,50544662
Bare land compacted	0,056	0,047	-16,07142857
Bare land rocks and gravel	0,0401	0,0342	-14,71321696
Railroads	0,0086	0,0082	-4,651162791
Field agricultural land on sandy soil	0,0012	0,0004	-66,66666667
Roads Unpaved	0	0,0014	
Total	**9,0641**	**6,0512**	

5. Discussion

5.1 Justification for Infiltration Rate Selection and Estimations

To define a consistent range of infiltration rates across SLCs, the Ksat values from the Green-Ampt parameter table were used as a foundational reference (Rawls & Brakensiek, 1982; Rawls et al., 1982; Gowdish & Muñoz-Carpena, 2009). This table provides general minimal and maximal infiltration for sandy, silty, and clay soils. Within these boundaries, infiltration rates for specific SLCs were sourced from scientific literature and the SWIG database (Rahmati et al. 2018), prioritizing data where land use and soil type were both specified.

In cases where observed values exceeded the Green-Ampt range, such as rain gardens with infiltration rates of 241–245 mm/hr (Venvik & Boogaard 2020), adjustments were made to align them with the defined framework. This ensured consistency across the model while preserving relative differences between land cover types. Furthermore, adjustments were made where the observed infiltration rate covers a single value. This is the case for *Building- Green roof*, which has an infiltration of 37.5 mm/hr according to Bondì et al. (2023) Based on this value, -10% and 10% were calculated in order to specify a range of infiltration.

Where no reliable values were available, logical estimations were made based on comparable SLCs with known values. These estimations were guided by land cover function (e.g., forest vs. bare land), similarity to other classified surfaces, and the expected infiltration behavior of the corresponding soil group. Particular effort was made to ensure infiltration rates for natural land cover types across all soil groups are covered, to allow for robust and comparative flood modelling. Nevertheless, further research on infiltration rates is needed in order to replace estimations with scientific findings.

The SWIG database includes relatively few observations from Sweden or similar climate conditions. Additionally, infiltration rate data derives from 12 different measurement methods, which lack detailed information on key parameters, such as the applied water volume to the testing and duration to reach saturated infiltration. These inaccuracies led to uncertainty in the absolute infiltration values and highlight the need for a standardized methodology when applying infiltration data in a local context like Sweden.

In Table 5, the Manning coefficient for OBJECT ID 25 and 32 (no value) has been set to 0.001. This is due to the reason that the Manning coefficient cannot be zero, as that would mean no runoff would be generated.

The infiltration rate of water has been set to 0 mm/hr. The reason behind this decision is that in flood modelling, there is an issue with water bodies when working with DEM as ground layer, as the DEM considers the depth of water bodies and not their volume and volume capacity (more in 5.3). Setting the infiltration of water to 0 mm/hr allows for investigation of the accumulated water volume (water depth and size) caused by flood simulation on top of water bodies.

5.2 Applicability of the soil land cover infiltration table

The soil land cover infiltration table covers 24 different classes and thereby offers a wide range of usage, for example, in Sweden and other countries with similar climate conditions. The inclusion of land cover classes like agricultural fields, grass, forests, and various urban surfaces makes the table useful for urban planners, municipalities, and hydrological modelers working with land use settings.

However, the SLC table has been applied to a small coastal area in Southern Sweden, which is not representative of the whole of Sweden. Certain land cover and soil conditions are not included yet. Snow and Ice as land use classes, as well as permafrost conditions, are not represented in the table, which limits its applicability in northern Sweden and similar climatic environments. To extend the usage to the whole of Sweden, further research is needed to quantify infiltration rates and Manning coefficients for snow and ice, and how to incorporate the behavior of permafrost soils.

At the current state, the SLC table contains many estimated infiltration rate ranges (Table 5). Future studies should replace those estimates with in-field measured infiltration rates to strengthen the accuracy and reliability of the table.

Despite these limitations, the table's content and structure could allow usage beyond Sweden. Regions such as Denmark, northern Germany, and the Netherlands, if local conditions share similar land cover classes, soil and climate conditions, the SLC table could serve as a preliminary guideline for infiltration rates and flood modelling. However, users would need to decide on infiltration rates due to their local context and/or adjust values based on local data, when available.

5.3 Interpretation of the results from flood simulations

Soil land cover types with high infiltration experienced fluctuating differences in flood extent in the study area from minimum to maximum infiltration. In contrast, areas with low infiltration remained consistently flood-prone in both simulations (Table 7). Amongst SLCs with high infiltration are sandy soils, and for low infiltration, clay soils. These findings partially align with those of Saco et al. (2021), who observed that sandy soils reduce runoff primarily under high infiltration conditions, whereas clay soils consistently generate runoff regardless of the infiltration scenario. This emphasizes that infiltration rates are influenced not only by soil type but also by the interaction between topography, soil properties, and land use.

In Figures 7, 8, and 9, we observe water depth across various water bodies within Lomma watershed. However, the water depth in water bodies does not directly indicate if the area is flooded or not. This is most likely due to the reason that the DEM, which has been set to ground layer for simulations, doesn’t cover information about the potential water capacity of these water bodies and simply represents the ground of the waterbodies as elevation. To make further studies more precise, information like this should be built into DEM models to allow easy access to reliable flood modelling.

The simulation scenarios of the rainfall event using minimum and maximum infiltration rates for different SLCs highlight the significant influence of infiltration in combination with topography. This is particularly evident in the Lomma watershed, where the SLC "Forest or high vegetation on sandy soils"—despite having one of the highest infiltration rates (Table 2)—is located primarily in topographic depressions. As a result, it experiences the greatest extent of maximum water depths exceeding 30 cm under minimum infiltration conditions, which, according to Taramelli et al. (2022), can pose severe hazards, depending on water velocity. However, when maximum infiltration is applied, the affected area is reduced by approximately 93% (Table 7). This case study illustrates not only the critical impact of infiltration rates on flood modeling but also the importance of applying them thoughtfully, accounting for the interaction between land cover and terrain.

Furthermore, most flooded areas are located in topographic depressions rather than on slopes, which supports the findings of Fox et al. (1997). This example highlights the influence of infiltration rate ranges on flood extent, but also emphasizes that such rates must be applied with careful consideration, as their effects can vary significantly depending on local terrain and soil characteristics.

The study area is generally well-prepared for rainfall events that occur with a frequency of once every ten years, indicating its capacity to manage significant precipitation without experiencing highly hazardous flood depths. During such events, it has been observed that most regions within the area may experience flooding levels approaching 10 centimeters. Although these flood depths can result in certain damages, such as localized disruptions to transportation and minor property impacts, the overall effects are expected to be relatively minor in scale. The infrastructure in place appears to mitigate more severe consequences, ensuring that the community can recover quickly from these temporary inundations. However, from a planning perspective, it is essential to focus on preserving or enhancing infiltration in areas prone to flooding. In this case, areas where the maximum water depth exceeded the threshold of 10 centimeters should be improved. This could be done by emphasizing rain gardens, increasing vegetation cover, or replacing sealed surfaces with permeable materials can significantly reduce runoff and mitigate flood risks. Furthermore, simulations of 100-year return rainfall should be carried out, as the frequency of such events is likely to increase in southern Sweden (Slater et al. 2021).

6. Conclusions

This study demonstrates the significant impact of soil and land cover infiltration rates on flood modelling outcomes. By developing a standardized soil land cover (SLC) infiltration rate table, including infiltration ranges and Manning coefficients, this work provides a valuable tool for urban planners, municipalities, and hydrological modelers seeking to perform realistic flood simulations. With the help of the workflow chart (Figure 5) and the SLC table, such users can easily perform flood analysis in their local context.

Reviewing the results from the SWIG database (Table 4), we see big differences in infiltration rates across and within land cover classes, which confirms the first hypothesis of this paper.

Applied to the Lomma watershed, the SLC infiltration table revealed that infiltration rates greatly influence flood extent, particularly in areas with high-permeability soils located in depressions. Flood-prone areas with SLCs on clay soils (low infiltration) remained largely unchanged between infiltration scenarios, while areas with SLCs on sandy soils (high infiltration) showed reductions in flood extent of up to 93% in high infiltration scenarios.

The findings of this thesis highlight the importance of accounting for soil type, land use, and topography when modelling infiltration and runoff in flood simulations. While most areas within the study area can handle a 10-year return rainfall event without severe flooding, localized improvements, such as increasing vegetated surfaces with higher infiltration SLCs or replacing sealed areas with permeable materials, can further reduce risk.

The table developed in this study can be adapted to similar climates in Sweden, Denmark, the Netherlands, or northern Germany, if local conditions are considered. However, future studies should conduct field measurements of infiltration rates to improve model accuracy and broaden its applicability.

Nevertheless, the developed soil land cover infiltration table represents a structured and comparative approach. The table provides a practical and flexible tool for flood modelling and land-use planning. Its adaptability to local and international settings enhances its value.

7. Limitations

This study is limited to flood simulations caused by a rainfall event. In the case of Lomma municipality, flood scenarios caused by sea water rise should be tied into rainfall events to give a comprehensive flood overview.

The results only focus on maximum water depth as an indicator of flood risk and extent. In order to carry out a deeper flood analysis, the water velocity needs to be considered. Data about the water velocity of the flood scenarios is available but could not be considered in this paper due to the limit of time.

In Figure 7, we see the overlay of the difference in maximum water depth between minimum and maximum infiltration. However, besides visualizing, it was not possible to extract precise statistics about how much of each soil land cover type was covered by how much water due to an unexpected error in ArcGIS Pro that could not be fixed in time. These statistics would have provided this study with a more in-depth analysis of how much each soil-land cover class is affected in both flood scenarios.

8. References

Amami, R., Ibrahimi, K., Sher, F., Milham, P., Ghazouani, H., Chehaibi, S., Hussain, Z. & Iqbal, H.M.N. (2021). Impacts of Different Tillage Practices on Soil Water Infiltration for Sustainable Agriculture. *Sustainability*, 13 (6), 3155. https://doi.org/10.3390/su13063155

Becker, P. (2021). Fragmentation, commodification and responsibilisation in the governing of flood risk mitigation in Sweden. *Environment and Planning C: Politics and Space*, 39 (2), 393–413. https://doi.org/10.1177/2399654420940727

Bondì, C., Concialdi, P., Iovino, M. & Bagarello, V. (2023). Assessing short- and long-term modifications of steady-state water infiltration rate in an extensive Mediterranean green roof. *Heliyon*, 9 (6), e16829. https://doi.org/10.1016/j.heliyon.2023.e16829

Fox, D.M., Bryan, R.B. & Price, A.G. (1997). The influence of slope angle on final infiltration rate for interrill conditions. *Geoderma*, 80 (1), 181–194. https://doi.org/10.1016/S0016-7061(97)00075-X

Fu, B., Chen, L., Ma, K., Zhou, H. & Wang, J. (2000). The relationships between land use and soil conditions in the hilly area of the loess plateau in northern Shaanxi, China. *CATENA*, 39 (1), 69–78. https://doi.org/10.1016/S0341-8162(99)00084-3

Gowdish, L. & Muñoz-Carpena, R. (2009). An improved Green-Ampt infiltration model for sloping terrain. *Transactions of the ASABE*, 52 (1), 55–68

Madsen, H., Lawrence, D., Lang, M., Martinkova, M. & Kjeldsen, T.R. (2014). Review of trend analysis and climate change projections of extreme precipitation and floods in Europe. *Journal of Hydrology*, 519, 3634–3650. https://doi.org/10.1016/j.jhydrol.2014.11.003

Malmö stad (2024). *Tio år efter skyfallet Arvid*. [text]. https://malmo.se/Aktuellt/Artiklar-Malmo-stad/2024-08-27-Tio-ar-efter-skyfallet-Arvid.html [2025-05-03]

Mueller, G.D. & Thompson, A.M. (2009). The Ability of Urban Residential Lawns to Disconnect Impervious Area from Municipal Sewer Systems. *JAWRA Journal of the American Water Resources Association*, 45 (5), 1116–1126. https://doi.org/10.1111/j.1752-1688.2009.00347.x

Ni, X., Huang, H., Dong, W., Chen, C., Su, B. & Chen, A. (2021). *Scenario Prediction and Crisis Management for Rain-induced Waterlogging Based on High-precision Simulation*. https://www.researchgate.net/publication/350531195_Scenario_Prediction_and_Crisis_Management_for_Rain-induced_Waterlogging_Based_on_High-precision_Simulation

Poschlod, B., Ludwig, R. & Sillmann, J. (2021). Ten-year return levels of sub-daily extreme precipitation over Europe. *Earth System Science Data*, 13 (3), 983–1003. https://doi.org/10.5194/essd-13-983-2021

Rahmati, M., Weihermüller, L. & Vereecken, H. (2018). Soil Water Infiltration Global (SWIG) Database. *Supplement to: Rahmati, M et al. (2018): Development and Analysis of Soil Water Infiltration Global Database. Earth System Science Data*. PANGAEA. https://doi.org/10.1594/PANGAEA.885492

Rawls, W.J. & Brakensiek, D.L. (1982). Estimating soil water retention and hydraulic properties. In: *Advances in Soil Science*. Springer. 293–299.

Rawls, W.J., Brakensiek, D.L. & Saxton, K.E. (1982). Estimation of soil water properties. *Transactions of the ASAE*, 25 (5), 1316–1320

Roseen, R.M., Ballestero, T.P., Houle, J.J., Briggs, J.F. & Houle, K.M. (2012). Water Quality and Hydrologic Performance of a Porous Asphalt Pavement as a Storm-Water Treatment Strategy in a Cold Climate. *Journal of Environmental Engineering*, 138 (1), 81–89. https://doi.org/10.1061/(ASCE)EE.1943-7870.0000459

Sauer, T.J., Logsdon, S.D., Van Brahana, J. & Murdoch, J.F. (2005). Variation in infiltration with landscape position: Implications for forest productivity and surface water quality. *Forest Ecology and Management*, 220 (1), 118–127. https://doi.org/10.1016/j.foreco.2005.08.009

Sayl, K.N., Afan, H.A., Muhammad, N.S. & ElShafie, A. (2017). Development of a Spatial Hydrologic Soil Map Using Spectral Reflectance Band Recognition and a Multiple-Output Artificial Neural Network Model. Water Resources Management/Remote Sensing and GIS. https://doi.org/10.5194/hess-2017-13

Scalgo (2025). *Soil properties – SCALGO Live Documentation*. https://scalgo.com/en-US/scalgo-live-documentation/soil-vegetation-atmosphere-properties/soil/properties

SGU (2024). *Jordartsdata*. https://www.sgu.se/produkter-och-tjanster/geologiska-data/jordarter--geologiska-data/jordartsdata/ [2025-05-03]

Shukla, M.K., Lal, R., Owens, L.B. & Unkefer, P. (2003). LAND USE AND MANAGEMENT IMPACTS ON STRUCTURE AND INFILTRATION CHARACTERISTICS OF SOILS IN THE NORTH APPALACHIAN REGION OF OHIO. *Soil Science*, 168 (3), 167. https://doi.org/10.1097/01.ss.0000058889.60072.aa

Slater, L., Villarini, G., Archfield, S., Faulkner, D., Lamb, R., Khouakhi, A. & Yin, J. (2021). Global Changes in 20-Year, 50-Year, and 100-Year River Floods. *Geophysical Research Letters*, 48 (6), e2020GL091824. https://doi.org/10.1029/2020GL091824

Sun, D., Yang, H., Guan, D., Yang, M., Wu, J., Yuan, F., Jin, C., Wang, A. & Zhang, Y. (2018). The effects of land use change on soil infiltration capacity in China: A meta-analysis. *Science of The Total Environment*, 626, 1394–1401. https://doi.org/10.1016/j.scitotenv.2018.01.104

S.V.T. Nyheter (2024). *Prislappen för skyfallet i Gävle 2021 landar på mer än väntat*. *SVT Nyheter*. https://www.svt.se/nyheter/lokalt/gavleborg/prislappen-for-skyfallet-i-gavle-2021-landar-pa-mer-an-vantat [2025-05-03]

SWECO (2009). *Översvämningskartering av Höje å genom Lomma kommun samt analys av stigande havsnivå*. Lomma Municipality. https://lomma.se/download/18.2f61993515a5f2b1e314b24/1488815379878/Översvämningskartering%20av%20Höje%20å%20genom%20Lomma%20kommun.pdf

Taramelli, A., Righini, M., Valentini, E., Alfieri, L., Gatti, I. & Gabellani, S. (2022). *Building-scale flood loss estimation through enhanced vulnerability pattern characterization: application to an urban flood in Milano, Italy*. https://doi.org/10.5194/egusphere-2022-225

U.S. Army Corps of Engineers (2021). HEC-RAS River Analysis System: 2D Modeling User's Manual. Version 5.0. [2025-05-03]

Venvik, G. & Boogaard, F.C. (2020). Infiltration Capacity of Rain Gardens Using Full-Scale Test Method: Effect of Infiltration System on Groundwater Levels in Bergen, Norway. *Land*, 9 (12), 520. https://doi.org/10.3390/land9120520

Vieira Passos, M., Kan, J.-C., Destouni, G., Barquet, K. & Kalantari, Z. (2024). Identifying regional hotspots of heatwaves, droughts, floods, and their co-occurrences. *Stochastic Environmental Research and Risk Assessment*, 38 (10), 3875–3893. https://doi.org/10.1007/s00477-024-02783-3

Wikantyasa, B. & Kusumandari, A. (2022). The infiltration capacity and rate at the grass, building yard and green open space areas of Universitas Gadjah Mada campus. *IOP Conference Series: Earth and Environmental Science*, 959 (1), 012046. https://doi.org/10.1088/1755-1315/959/1/012046

Ye, A., Zhou, Z., You, J., Ma, F. & Duan, Q. (2018). Dynamic Manning's roughness coefficients for hydrological modelling in basins. *Hydrology Research*, 49 (5), 1379–1395. https://doi.org/10.2166/nh.2018.175

Yimer, F., Messing, I., Ledin, S. & Abdelkadir, A. (2008). Effects of different land use types on infiltration capacity in a catchment in the highlands of Ethiopia. *Soil Use and Management*, 24 (4), 344–349. https://doi.org/10.1111/j.1475-2743.2008.00182.x

Acknowledgements

Big thanks to my supervisor Abdulghani Hasan for guiding me through the project and for his patience. Special thanks to my parents and my brother Luca for your endless support in every situation. Without you I would have never made it this far. I love you.

Appendix 1

R-Studio code for filtering the SWIG database.

```
Soiltype_Landuse <- data %>%
  filter(!is.na(Ksat), !is.na(`Landuse (classifed)`)) %>%
  mutate(Ksat = as.numeric(Ksat)) %>%
  group_by(`Texture Class`, `Landuse (classifed)`) %>%
  summarise(
    n = n(),
    mean_ksat = mean(Ksat, na.rm = TRUE),
    median_ksat = median(Ksat, na.rm = TRUE)
  )
```

Appendix 2

Field calculator code in ArcGIS Pro to categorise soil types into soil classes clay soils, silty soils, sandy soils and water.

```
var soil = $feature.JG2_TX;


if (soil == "Flygsand" || soil == "Isglvssediment, sand" || soil == "Isllvssediment, sand" ||
   soil == "Postglacial finsand" || soil == "Postglacial sand" || soil == "Sandig mor" ||
   soil == "Svallsediment, grus" || soil == "Svlmsediment, sand" || soil == "Is" || soil == "Fyllning") {
   return "Sandy soils";
}
else if (soil == "Glacial lera" || soil == "Lerig moran" || soil == "Lerig moren" || soil == "Lerig morin" ||
      soil == "Morinfinlera" || soil == "Moringrovlera" || soil == "Mormnfinlera" || soil == "Mormngrovlera" ||
      soil == "Mormnlera" || soil == "Postglacial finlera" || soil == "Postglacial grovlera" || soil == "Postglacial lera") {
   return "Clay soils";
}
else if (soil == "Glacial grovsilt--finsand" || soil == "Isllvssediment" ||
      soil == "Svgmsediment, ler--silt" || soil == "Svlmsediment, grovsilt--finsand" || soil == "Svlmsediment, ler--silt") {
   return "Silty soils";
}
```

```
else if (soil == "Gyttja" || soil == "Gyttjelera (eller lergyttja)" || soil == "Karrtorv"
|| soil == "Korrtorv") {

   return "Mire";

}

else if (soil == "Vatten") {

   return "Water";

}

else {

   return "Other";

}
```

Publishing and archiving

Approved students' theses at SLU can be published online. As a student you own the copyright to your work and in such cases, you need to approve the publication. In connection with your approval of publication, SLU will process your personal data (name) to make the work searchable on the internet. You can revoke your consent at any time by contacting the library.

Even if you choose not to publish the work or if you revoke your approval, the thesis will be archived digitally according to archive legislation.

You will find links to SLU's publication agreement and SLU's processing of personal data and your rights on this page:

- https://libanswers.slu.se/en/faq/228318

☒ YES, I, Joshua Friese, have read and agree to the agreement for publication and the personal data processing that takes place in connection with this

☐ NO, I/we do not give my/our permission to publish the full text of this work. However, the work will be uploaded for archiving and the metadata and summary will be visible and searchable.